PHYSICAL REVIEW B **86**, 180404(R) (2012)

Emergence of topological Hall effect from fanlike spin structure as modified by Dzyaloshinsky-Moriya interaction in MnP

Y. Shiomi,[1,*] S. Iguchi,[1,2] and Y. Tokura[1,3]

[1]*Department of Applied Physics, University of Tokyo, Tokyo 113-8656, Japan*

[2]*Institute for Materials Research, Tohoku University, Sendai 980-8577, Japan*

[3]*Cross-Correlated Materials Research Group (CMRG)/Correlated Electron Research Group (CERG), RIKEN Advanced Science Institute (ASI), Wako 351-0198, Japan*

(Received 16 June 2012; revised manuscript received 21 October 2012; published 15 November 2012)

A nontrivial Hall effect has been observed as an anomaly of the Hall conductivity in the magnetization process in a typical itinerant helimagnet MnP. Since the Dzyaloshinsky-Moriya interaction slightly modulates the spin structure, the anomaly is identified only in the specific magnetic (fanlike) phase that can have finite scalar spin chirality. The decrease in the magnitude of the anomaly as observed by doping Co is well accounted for in terms of the topological Hall effect arising from the spin-chirality-induced Berry phase in real space. A fictitious magnetic flux in real space is estimated to be ∼1 T, which is consistent with the small modulation of the spin structure.

DOI: 10.1103/PhysRevB.86.180404 PACS number(s): 75.25.−j, 75.47.−m, 72.15.−v, 72.20.My

Helimagnetic materials have been attracting special interest because of the recent discovery of spin-charge-coupled phenomena via noncollinear spin order. For example, ferroelectricity is driven by spiral-spin order as discovered in $TbMnO_3$ (Ref. 1) and many other helimagnetic insulators.[2–4] Another example is a topological Hall effect (THE) as observed in a phase with the lattice formation of a skyrmion, stabilized by the Dzyaloshinsky-Moriya (DM) interaction.[5–7] While the Hall effect in magnets is usually induced by the Lorentz force (normal Hall effect) and the spin-orbit interaction [anomalous Hall effect (AHE)], the scalar spin chirality $[\boldsymbol{S}_i \cdot (\boldsymbol{S}_j \times \boldsymbol{S}_k)]$ hosted by each skyrmion also drives the Hall current, showing THE. The magnetic field (H) dependence of the total Hall conductivity (σ_H) is then expressed by[7]

$$\sigma_H(H) = R_0\{\sigma(H)\}^2\mu_0 H + R_s\{\sigma(H)\}^{\alpha} M(H) + \sigma_H^T(H), \tag{1}$$

where the first, second, and third terms indicate the normal, anomalous, and topological Hall conductivity, respectively. R_0, R_s, σ, and M indicate Hall coefficients for normal and anomalous Hall effects, the longitudinal conductivity, and magnetization, respectively. For anomalous Hall conductivity, $\alpha = 0$ and $\alpha = 1$ are predicted for intrinsic (spin-orbit-induced Berry phase) and extrinsic (skew-scattering) mechanisms, respectively.[8] For the intrinsic AHE, the Berry curvature of electronic Bloch states acts as a fictitious magnetic flux in momentum space ($\boldsymbol{k}$ space). Likewise, conduction electrons acquire the Berry phase while passing through the skyrmion lattice as the origin of THE.

For THE to be observed, the summation of scalar spin chirality over the whole lattice sites needs to be nonzero; however, this condition is believed to be rarely satisfied in simple helimagnets, because the effective flux cancels out due to the translational lattice symmetry in helimagnets which have one magnetic atom in a unit cell, even though a noncoplanar spin structure is realized in applied H.[9] Theoretically, two mechanisms of THE have been proposed: real ($\boldsymbol{r}$)-space and $\boldsymbol{k}$-space pictures. They take a dominant role in $l \ll \lambda_S$ and $l \gg \lambda_S$, respectively, where l and λ_S are the electron mean free path and length scale of the topological spin texture, respectively.[9,10] In the $\boldsymbol{r}$-space picture, the scalar spin chirality summed over $\boldsymbol{r}$-space spins, namely, the skyrmion number, is directly linked to THE. In the skyrmion lattice case, the fictitious magnetic flux in $\boldsymbol{r}$ space is estimated as $B_{\mathrm{eff}} \approx \pm(h/e)\lambda_S^{-2}$ in the case of strong coupling between conduction electrons and the underlying local spins, where h and e are Planck's constant and the elementary charge, respectively. The magnitude of the topological Hall resistivity (ρ_H^T) is almost consistent with $R_0 B_{\mathrm{eff}}$ for MnSi (Ref. 5) and MnGe.[7] On the other hand, the $\boldsymbol{k}$-space picture is related to the Berry phase in $\boldsymbol{k}$ space. For noncoplanar spin order on a kagome[11] or distorted fcc[12] lattice, a multiband structure resulting from more than two atoms and/or orbitals in the unit cell is responsible for the THE in the case of strong coupling. The Hall effect induced by this mechanism has been reported for pyrochlore magnets $Nd_2Mo_2O_7$ (Ref. 13) and $Pr_2Ir_2O_7$.[14] One crucial difference between the $\boldsymbol{r}$- and $\boldsymbol{k}$-space pictures appears in the scattering-rate ($1/\tau$) dependence of σ_H^T (or ρ_H^T).[10] The $\boldsymbol{k}$-space picture suggests that σ_H^T is independent of τ, similarly to the intrinsic AHE. By contrast, the $\boldsymbol{r}$-space picture predicts that $\rho_H^T \approx \sigma_H^T/\sigma^2$ is constant as a function of τ, which was actually observed for MnGe.[7] In this Rapid Communication, we show that the Hall effect in an itinerant helimagnet MnP under $H||b$ cannot be explained by conventional (normal plus anomalous) Hall terms alone, and but that the explicit contribution from THE has to be taken into account. The σ_H^T in $H||b$ decays in proportion to τ^2 along with an increase of ρ by doping Co into the Mn site, validating the $\boldsymbol{r}$-space picture for the observed THE.

Manganese phosphide (MnP) is one of the typical itinerant helimagnets and its magnetic properties have been intensively investigated for decades,[15–20] but a complete understanding is yet to be attained.[21,22] MnP has an orthorhombic crystal structure ($B31$). The lattice constants are $a_0 = 5.918$ Å, $b_0 = 5.258$ Å, and $c_0 = 3.172$ Å.[23] The unit cell contains four Mn atoms and four P atoms. As shown in Fig. 1(a), Mn zigzag chains within the ab plane run along the b axis. At

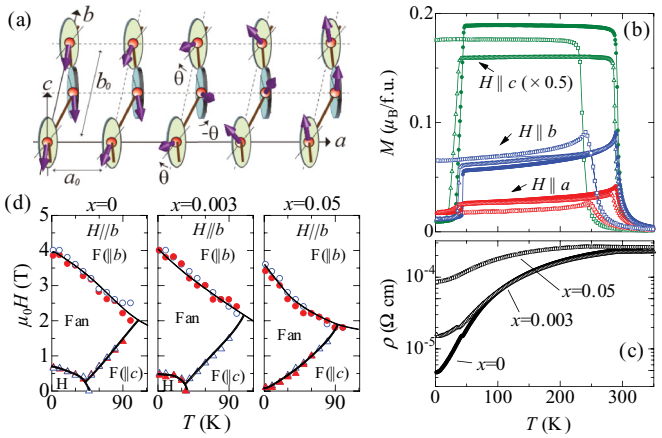

FIG. 1. (Color online) (a) A schematic view of the helical spin structure of MnP in the helimagnetic (H) state in zero field. Temperature (T) dependence of (b) magnetization (M) at a magnetic field of $\mu_0 H = 0.1$ T along the a, b, or c axis, and (c) resistivity (ρ) in zero field, for $x = 0$ (solid circles), $x = 0.003$ (open triangles), and $x = 0.05$ (open squares). (d) Low-temperature magnetic-phase diagrams in $H||b$ for $x = 0$, $x = 0.003$, and $x = 0.05$. H, Fan, and F indicate the helimagnetic, fan, and ferromagnetic phases, respectively. Phase boundaries [solid and open circles (triangles)] are determined by M-H and ρ-H measurements, respectively.

zero field, the ferromagnetic (F) and helimagnetic (H) phases have been reported between $T_C = 291$ K and $T_h = 47$ K and below T_h, respectively.[15–17] In the F phase, the Mn spins are aligned along the c axis above $T^* = 282$ K,[18] but they slightly reorient toward the b axis below T^* ($T_h < T < T^*$).[16,17] In the H phase below T_h, the spin spiral propagates along the a axis with a period of about $9a_0$ at 4.2 K.[19,20] The Mn spins are almost aligned collinearly within the bc plane, but the helical plane is slightly rotated ($\theta \sim 2°$–$6°$) around the c axis to the a direction by the DM interaction, as shown in Fig. 1(a).[17] The small a component is antiferromagnetic along the b axis, but ferromagnetic along the c axis. The magnetic property of Co-substituted MnP was also investigated.[24,25] CoP is a Pauli paramagnetic metal with the same $B31$ structure, and T_C decreases monotonically by doping Co in proportion to the difference in the number of valence electrons between CoP and MnP.[24]

The single crystals of $Mn_{1-x}Co_xP$ ($x = 0$, 0.003, and 0.05) were grown by a Bridgman method. In Fig. 1(b), we show the temperature (T) dependence of the magnetization (M) for $Mn_{1-x}Co_xP$ in $\mu_0 H = 0.1$ T applied along the a, b, or c axis. For $x = 0$, two sharp transitions are observed at $T_C \approx 290$ K and $T_h \approx 45$ K.[26] By doping a slight amount of Co ($x = 0.003$), both the transition temperatures become lowered by about 5 K. For the 5% doped sample, the T_C decreases down to 240 K, and remarkably the helimagnetic transition is no longer observed. The longitudinal resistivity (ρ) in zero field for these samples is shown in Fig. 1(c). While the magnetic anisotropy is strong, ρ is isotropic, being consistent with a former report.[27] A ρ of $x = 0$ shows good metallicity ($d\rho/dT > 0$) below T_C; the residual ρ is as low as 5 $\mu\Omega$ cm. By doping Co, the residual ρ increases monotonically. An anomaly corresponding to the helimagnetic transition is observed at 40–45 K for $x = 0$ and $x = 0.003$, while it is no longer observed in $x = 0.05$. This is in accord with the result of M in $\mu_0 H = 0.1$ T [Fig. 1(b)], indicating the absence of the H phase as shown in Fig. 1(d).

We investigate the magnetic phase diagrams in $H||b$ for all the samples by measuring the H dependence of M and ρ [Fig. 1(d)]. When H is applied along the b axis for MnP, a fan phase, in which the magnetic moments do not show a full rotation but oscillate as a *fan*, appears in the intermediate H region below about 100 K [Fig. 1(d)].[25,28] The period of the fan structure for MnP as determined by the neutron diffraction study is $18a_0$ at 77 K in 1 T,[29] and varies with H and T.[30] By doping Co, the H phase region becomes narrower, while the size of the fan phase hardly changes.[25] The magnetic transitions from H or F($||c$) to the fan phase are of the first order, while those from F($||c$) or fan to F($||b$) ones are of the second order.[25] Although the slight modulation of helical spin structure by a DM interaction has been reported only in zero field, a similar modulation is expected in applied H as well.[17] If so, it will affect the Hall effect through the scalar-spin-chirality mechanism, as argued below. Conversely, the Hall effect measurement in MnP gives useful information on its veiled magnetism, in addition to recent interest on the topological transport in helimagnets.

In Fig. 2, we show the H dependence of the Hall conductivity (σ_H) under $H||b$ below 100 K for all the samples. We measured the Hall resistivity ($\rho_H \equiv E_H/J$, where E_H and J are the Hall electric field and applied electric current density, respectively) within the ac plane in $H||b$, and transformed it into Hall conductivity by the relation where $\sigma_H = \rho_H/\rho^2$. Corresponding to the magnetic transitions driven by H, σ_H shows nontrivial H dependence; a dip is observed in the fan phase for $x = 0$ [Figs. 2(b)–2(e)] and $x = 0.003$ [Figs. 2(g)–2(j)]. This unconventional behavior in the fan phase ($\sim 10^{-8}$ Ω cm in ρ_H for MnP) is recognized here. As described above, the H dependence of σ_H is generally described by Eq. (1). In Fig. 2, we estimate the conventional

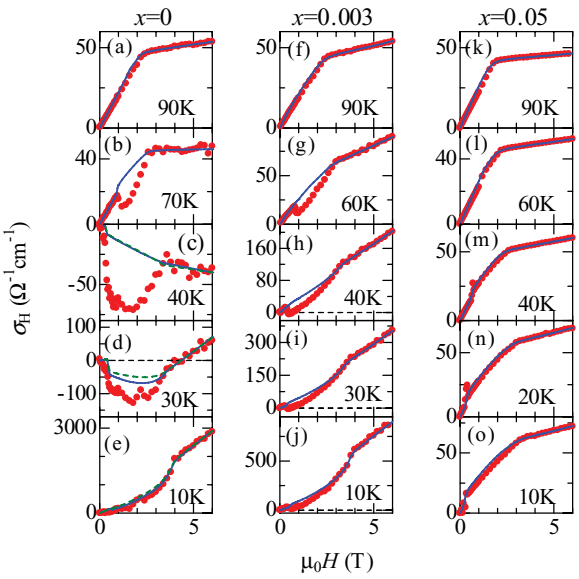

FIG. 2. (Color online) Hall conductivity (σ_H, dots) as a function of magnetic field (H) applied along the b axis for $x = 0$, $x = 0.003$, and $x = 0.05$. The solid (dashed) lines are the fitted results assuming $\alpha = 0$ ($\alpha = 1$) (see text).

terms (normal plus anomalous Hall terms) by Eq. (1) without the third term. The solid (blue) lines indicate the estimated conventional terms of σ_H assuming the Berry-phase-induced (intrinsic) AHE ($\alpha = 0$).[31] For $x = 0$, below 50 K, where the resistivity is below 10 $\mu\Omega$ cm, we also try to fit σ_H in terms of the skew scattering ($\alpha = 1$, green dashed lines).[31] As shown in Fig. 2, however, the estimates with taking into account both the intrinsic (Berry phase) and extrinsic (skew-scattering) terms cannot explain the H dependence of σ_H in the fan phase as far as the H-independent R_0 and R_s are assumed; on the contrary, the analysis under the same assumptions can satisfactorily fit the σ_H in the high-T region [Figs. 2(a), 2(f), and 2(k)]. As the origin for this deviation in the fan phase, one may consider a possible change of R_0 and R_s across the first-order transitions from H or F($||c$) to the fan phase. Judging from the well fitted σ_H by conventional terms in both F($||c$) and F($||b$) phases with the same R_0 and R_s [Figs. 2(b), 2(g), and 2(h)], however, the values of R_0 and R_s are considered to remain unchanged across the first-order transition. Therefore, we cannot explain the observed dip structure in the fan phase by conventional Hall terms, and need another contribution with a negative sign to the Hall effect, which is assigned as the THE.

We estimate the possible topological Hall conductivity (σ_H^T) as the difference between the σ_H and the fitted curves, as shown in the form of a contour map for $x = 0$ and $x = 0.003$ (Fig. 3). Here, we simulate the conventional, i.e., non-THE, component with $\alpha = 0$ (intrinsic origin) in $T \geqslant 50$ K for $x = 0$ and in the whole T region for $x = 0.003$ and 0.05. For $x = 0$, in the very low resistive ($\rho < 10\ \mu\Omega$ cm) region of $T < 50$ K, the non-THE component with $\alpha = 1$ (skew-scattering process) is adopted because σ_H in a high-H region shows a complex change with T below 50 K [Figs. 2(c)–2(e)] which should be interpreted as signaling the skew-scattering contribution.[31,32] The negative σ_H^T is observed in the fan and H phases for $x = 0$ and in the fan phase for $x = 0.003$ (Fig. 3). In the H phase of MnP, large σ_H^T might be merely an artifact because of very low ρ and $\rho_H (\leqslant 2$ nΩ cm); hereafter we will focus on σ_H^T in the fan phase. $|\sigma_H^T|$ decreases monotonically with increasing T or Co concentration [see also Fig. 2(o)]. Thus, σ_H^T is observed in

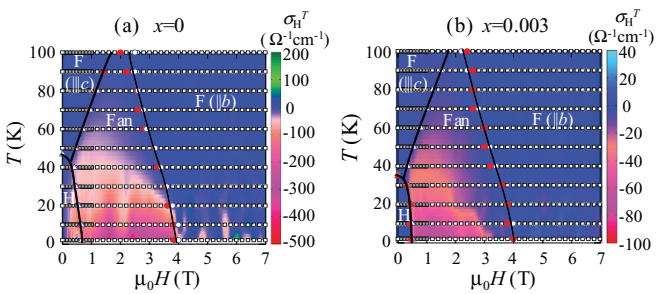

FIG. 3. (Color online) Contour maps of the topological Hall conductivity (σ_H^T) measured in $H||b$ in the plane of T and $\mu_0 H$ for (a) $x = 0$ and (b) $x = 0.003$. Open squares indicate the measured points of Hall conductivity. Abbreviations mean the same as those in Fig. 1(d). Nonzero σ_H^T in the F($||b$) phase especially at low T's is not essential but merely an artifact; this is due to the error of the estimation of ρ_H^T amplified via very low ρ ($<10\ \mu\Omega$ cm) in the calculation of $\sigma_H^T = \rho_H^T/\rho^2$.

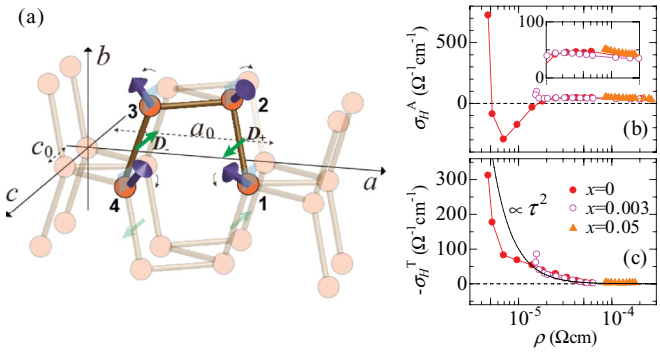

FIG. 4. (Color online) (a) Schematic illustration of the noncoplanar spin structure expected in the presence of a DM interaction. Labels 1–4 indicate four Mn sites in a unit cell. The spin modulation by the DM interaction [$\boldsymbol{D}_\pm = (0,0,\pm D)$, green arrows] between the nearest-neighboring Mn-1 and Mn-2 sites and between the nearest-neighboring Mn-3 and Mn-4 ones is assumed. (b) Anomalous Hall conductivity (σ_H^A) at 7 T ($||b$) and (c) topological Hall conductivity (σ_H^T) at 1.4 T ($||b$) as a function of longitudinal resistivity ρ for $x = 0$ (solid circles), $x = 0.003$ (open circles), and $x = 0.05$ (solid triangles). The inset to (b) shows the magnified view of σ_H^A in the region $2 \times 10^{-5}\ \Omega\,\text{cm} \leqslant \rho \leqslant 2 \times 10^{-4}\ \Omega\,\text{cm}$.

the state with a noncollinear spin structure, and its magnitude decreases with the increase of scattering rate (τ^{-1}).

The Hall effect measurement strongly suggests the noncoplanar spin structure endowed with the scalar spin chirality in the fan phase, although reports on spin structure modulation by the DM interaction in applied H are lacking. We illustrate in Fig. 4(a) the schematic view of the noncollinear spin structure, which is anticipated to be realized by a DM interaction. Here, the four Mn sites in a unit cell are labeled as Mn-1, Mn-2, Mn-3, and Mn-4 in Fig. 4(a). Since the tilting toward the a axis by the DM interaction is alternating along both the a and b axes, the directions of the spins on the four Mn sites in a unit cell are different from each other, and three of them form a noncoplanar structure. Owing to such a noncoplanar spin structure on these Mn sites, the total scalar spin chirality should not vanish, and thus contribute to THE. Note that in the H phase the existence of oppositely oriented spins could cancel out the net scalar spin chirality. As described above, THE is characterized by the spin-chirality-induced Berry phase in either $\boldsymbol{r}$ or $\boldsymbol{k}$ space.[10] We investigate the $\rho(T)$ ($\propto\tau^{-1}$) dependence of anomalous Hall conductivity $\sigma_H^A(T)$ at 7 T and $\sigma_H^T(T)$ at 1.4 T in $H||b$ in Figs. 4(b) and 4(c), respectively. Below 10 $\mu\Omega$ cm, σ_H^A shows complex behavior due to the skew scattering,[32] while it keeps an almost constant value of $\sim$50 Ω^{-1} cm^{-1} above that [see the inset to Fig. 4(b) for a magnification], as predicted for the intrinsic mechanism. This is the reason why we adopted $\alpha = 0$ and $\alpha = 1$ [see Eq. (1)] to correct the magnetoresistance effect, depending on the T region for $x = 0$. On the other hand, $-\sigma_H^T$ ($=|\sigma_H^T|$) for the three samples decreases almost in proportion to ρ^{-2} ($\propto\tau^2$) with increasing ρ, which verifies the validity of the $\boldsymbol{r}$-space picture of THE.[10] The scattering-free nature of ρ_H^T even in a finite-T region stems from the topological nature of the electronic Bloch state. According to the theory of THE,[10] the $\boldsymbol{r}$-space Berry phase should show a primary contribution in $l \ll \lambda_S$. A previous study on the de Haas–van Alphen effect in MnP (Ref. 33)

determined the electron mass (m) and Fermi wavelength (k_F) in the fan phase: $m = 0.2m_0$ and $k_F = 1.0 \times 10^9$ m^{-1}, where m_0 is the free electron mass. The relaxation time τ around the crossover from the intrinsic to extrinsic AHE ($\rho \sim 10\ \mu\Omega$ cm) is estimated by[34] $\tau \approx \hbar/E_{SO} \approx 0.66$–$2.2 \times 10^{-14}$ s, where $\hbar$ and E_{SO} [≈30–100 meV (Refs. 34–36)] are the reduced Planck constant and the energy of the spin-orbit interaction, respectively. Then, we roughly estimate the mean free path $l = v_F\tau = (\hbar k_F/m)\tau$ as 38–127 Å for $x = 0$ at $\rho \sim 10\ \mu\Omega$ cm. On the other hand, the period of the fan structure for MnP is 12–$15a_0 = 70$–89 Å at 1.4 T according to the neutron diffraction measurement.[30] Therefore, l is almost comparable to λ_S around the intrinsic to extrinsic crossover of AHE ($\rho \sim 10\ \mu\Omega$ cm), and becomes well smaller than λ_S by doping Co, which certifies the $\boldsymbol{r}$-space picture of THE. From the fitted curves in Fig. 4(c), the fictitious magnetic flux of THE at 1.4 T is estimated as $(\sigma_H^T/\rho^{-2})/R_0 \sim 0.5$–1 T, which is as small as that in the skyrmion phase of a long-period (180 Å) helimagnet MnSi.[5] The fictitious flux at 3 T (not shown) is half of that at 1.4 T, corresponding to the decrease in the period of fan.[30] The small fictitious flux is consistent with the scalar spin chirality resulting from the slight spin modulation by the DM interaction.

In conclusion, we have found an unconventional Hall effect in H applied along the b axis for $Mn_{1-x}Co_xP$ ($x = 0$, 0.003, and 0.05). The unconventional term in σ_H is found to decay in proportion to τ^2 by doping Co, which is consistent with the $\boldsymbol{r}$-space picture on THE. The estimated fictitious flux is ∼1 T, suggesting that THE is caused by scalar spin chirality resulting from the noncoplanar spin structure due to the small tilting of the spin plane in the fan phase by a DM interaction. The emergence of noncoplanarity of spin texture or skyrmion number as assisted by the DM interaction may be ubiquitous in the helimagnetic state, where a similar THE will be found.

We acknowledge Y. Onose, Y. Taguchi, Y. Endo, and N. Nagaosa for fruitful discussions. This work was in part supported by the Grant-in-Aid for Scientific Research (Grants No. 20340086 and No. 22740220) and JSPJ Fellows, and by the Funding Program for World-Leading Innovate R&D on Science and Technology (FIRST program) on "Quantum Science on Strong Correlation."

*Present address: WPI Advanced Institute for Materials Research, Tohoku University, Sendai 980-8577, Japan.

[1] T. Kimura *et al.*, Nature (London) **426**, 55 (2003).
[2] S.-W. Cheong and M. Mostovoy, Nat. Mater. **6**, 13 (2007).
[3] Y. Tokura and S. Seki, Adv. Mater. **22**, 1554 (2010).
[4] T. Arima, J. Phys. Soc. Jpn. **80**, 052001 (2011).
[5] A. Neubauer, C. Pfleiderer, B. Binz, A. Rosch, R. Ritz, P. G. Niklowitz, and P. Boni, Phys. Rev. Lett. **102**, 186602 (2009).
[6] M. Lee, W. Kang, Y. Onose, Y. Tokura, and N. P. Ong, Phys. Rev. Lett. **102**, 186601 (2009).
[7] N. Kanazawa, Y. Onose, T. Arima, D. Okuyama, K. Ohoyama, S. Wakimoto, K. Kakurai, S. Ishiwata, and Y. Tokura, Phys. Rev. Lett. **106**, 156603 (2011).
[8] N. Nagaosa *et al.*, Rev. Mod. Phys. **82**, 1539 (2010).
[9] N. Nagaosa and Y. Tokura, Phys. Scr., T **146**, 014020 (2012).
[10] M. Onoda, G. Tatara, and N. Nagaosa, J. Phys. Soc. Jpn. **73**, 2624 (2004).
[11] K. Ohgushi, S. Murakami, and N. Nagaosa, Phys. Rev. B **62**, 6065(R) (2000).
[12] R. Shindou and N. Nagaosa, Phys. Rev. Lett. **87**, 116801 (2001).
[13] Y. Taguchi *et al.*, Science **291**, 2573 (2001).
[14] Y. Machida, S. Nakatsuji, Y. Maeno, T. Tayama, T. Sakakibara, and S. Onoda, Phys. Rev. Lett. **98**, 057203 (2007).
[15] E. E. Huber, Jr. and D. H. Ridgley, Phys. Rev. **135**, A1033 (1964).
[16] C. C. Becerra, J. Phys.: Condens. Matter **12**, 5889 (2000).
[17] T. Yamazaki *et al.*, arXiv:1106.4599.
[18] G. Felcher, J. Appl. Phys. **37**, 1056 (1966).
[19] J. Forsyth, S. Pickart, and P. Brown, Proc. Phys. Soc. **88**, 333 (1966).
[20] R. M. Moon, J. Appl. Phys. **53**, 1956 (1982).
[21] E. E. Rodriguez, C. Stock, K. L. Krycka, C. F. Majkrzak, P. Zajdel, K. Kirshenbaum, N. P. Butch, S. R. Saha, J. Paglione, and M. A. Green, Phys. Rev. B **83**, 134438 (2011).
[22] T. Koyama *et al.*, J. Phys. Soc. Jpn. **81**, 043701 (2012).
[23] S. Rundqvist, Acta Chem. Scand. **16**, 287 (1962).
[24] H. Fjellvåg, A. Kjekshus, A. Zięba, and S. Foner, J. Phys. Chem. Solids **45**, 709 (1984).
[25] A. Zięba, C. C. Becerra, H. Fjellvåg, N. F. Oliveira, Jr., and A. Kjekshus, Phys. Rev. B **46**, 3380 (1992).
[26] To detect the subtle transition at $T^* \approx 282$ K, an applied field as small as 1–10 Oe is needed (Ref. 16).
[27] T. Suzuki, J. Phys. Soc. Jpn. **25**, 646 (1968).
[28] T. Komatsubara, T. Suzuki, and E. Hirahara, J. Phys. Soc. Jpn. **28**, 317 (1970).
[29] Y. Ishikawa, T. Komatsubara, and E. Hirahara, Phys. Rev. Lett. **23**, 532 (1969).
[30] H. Obara *et al.*, J. Phys. Soc. Jpn. **49**, 928 (1980).
[31] T. Miyasato, N. Abe, T. Fujii, A. Asamitsu, S. Onoda, Y. Onose, N. Nagaosa, and Y. Tokura, Phys. Rev. Lett. **99**, 086602 (2007).
[32] Y. Shiomi, Y. Onose, and Y. Tokura, Phys. Rev. B **79**, 100404(R) (2009).
[33] M. Ohbayashi, T. Komatsubara, and E. Hirahara, J. Phys. Soc. Jpn. **40**, 1088 (1976).
[34] S. Onoda, N. Sugimoto, and N. Nagaosa, Phys. Rev. Lett. **97**, 126602 (2006); Phys. Rev. B **77**, 165103 (2008).
[35] Y. Yao, L. Kleinman, A. H. MacDonald, J. Sinova, T. Jungwirth, D. S. Wang, E. Wang, and Q. Niu, Phys. Rev. Lett. **92**, 037204 (2004).
[36] T. Naito, D. S. Hirashima, and H. Kontani, Phys. Rev. B **81**, 195111 (2010).